J. Cell. Mol. Med. Vol 13, No 9B, 2009 pp. 3110-3121

Encapsulated cargo internalized by fusogenic liposomes partially overlaps the endoplasmic reticulum

Roxana C. Mustata, Alina Grigorescu, Stefana M. Petrescu*

From the Institute of Biochemistry of Romanian Academy, Department of Molecular Cell Biology, Splaiul Independentei, Bucharest, Romania

Received: July 8, 2008; Accepted: January 28, 2009

Abstract

Few endocytosed ligands, including bacterial toxins and simian virus 40 (SV40) have been shown to reach the endoplasmic reticulum (ER) in mammalian cells. Using calcein and fluorescently labelled lactoferrin encapsulated in fusogenic liposomes we found that the cargo uses a microtubule-based pathway with ER delivery. Endocytic uptake of the lipid vesicles was cholesterol dependent in all cell lines tested, including the caveolin-1-deficient human hepatoma 7 cell line. The ligand was transported in non-caveosome organelles requiring acidic pH for maturation, but able to escape the lysosomal route. These organelles were not recycling endosomes either, as shown by the lack of co-localization with recycling transferrin. Co-localization with the ER-tracker, orange fluorescent protein with KDEL signal retention and cholera toxin in live microscopy revealed an ER distribution of the fluorescent ligand. Brefeldin A, which prevents Golgi-dependent retrograde trafficking, does not disrupt the cargo delivery to the ER. This new endocytic pathway making use of acidic endosome-like organelles is an alternative to the reported SV40 caveolae pathways. Exploiting a cellular route linking the cell surface to the ER, fusogenic liposomes may become efficient drug delivery vehicles for ER stress and diseases.

Keywords: fusogenic liposomes • endocytosis • acidic endosomes • drug delivery • endoplasmic reticulum • intracellular trafficking

Introduction

Protein molecules destined for the extracellular space are co-translationally isolated from cytosol by recruitment at the endoplasmic reticulum (ER). In contrast with the reducing environment of the cytoplasm, the ER lumen has an oxidizing milieu which is similar with what the secreted molecule encounters outside the cell [1, 2]. Once translation and quality control processes occurring within the ER lumen are completed, proteins are exported by the secretory pathway which links the ER to the plasma membrane [3, 4]. Although this secretory function of the ER is well documented, little is known about reverse pathways which transport extracellular molecules from the plasma membrane to the ER. These pathways maybe particularly important in the ER stress induced apoptosis, or in the homeostasis of cholesterol, for which receptor molecules are located within the ER [5–7]. ER-mediated phagocytosis is another example of ER targeting from outside the cell that has been recently proposed as an adaptation of intracellular pathogens to avoid destruction in host cells [8].

Living cells require a continuous supply of molecules that are internalized from the environment by multiple endocytic pathways. These routes may lead to lysosomes where the cargo is degraded. However, many toxins, viruses and lipid vesicles such as melanosomes and exosomes are able to escape the cell degradative pathways [9–12]. Lysosomes are bypassed by some endocytosed viruses that escape from endosomes in the cytoplasm through fusion pores generated at low endosomal pH. Remarkable strides have been made recently in tracing some bacterial toxins, but also viruses within the ER of the host cell. Indeed, some toxins, including cholera toxin, find their way to the ER after endocytosis, by taking the retrograde pathway starting from endosomes and passing through the Golgi to the ER [13]. Although some retrograde endocytic pathways are well characterized, the direct routes that transport molecules from the plasma membrane to the ER have only recently started to be deciphered. At least two viruses, simian virus 40 (SV40) and polyomavirus are targeted to the ER of the infected cell for processing and retrotranslocation in the cytoplasm [14, 15]. Interestingly, the internalized viruses are

*Correspondence to: S.M. PETRESCU,
Institute of Biochemistry of Romanian Academy,
Splaiul Independentei 296, 060031,
Bucharest, Romania.
Tel.: +4021 2239069
Fax: +4021 2239068
E-mail: Stefana.Petrescu@biochim.ro

doi:10.1111/j.1582-4934.2009.00724.x

transported to the ER *via* both caveolin-dependent and caveolin-independent pathways, depending, in part, on the host cell, but mostly on unknown factors.

Here we show that besides toxins and viruses, vesicle encapsulated ligands are selectively internalized and may as well find their way to the ER, avoiding cytoplasm exposure. We have dissected the pathway that drives a molecule encapsulated into a lipid vesicle from the extracellular space to the ER. Our data showed that an encapsulated cargo entering the cell through either a clathrin- or a non-clathrin non-caveolae mediated endocytosis takes a microtubule driven way requiring endosomal acidification that targets the ER.

Materials and methods

Reagents

Laboratory reagents and different inhibitors used to investigate liposome entry and traffic were from Sigma (St. Lois, MO, USA). Reagents for tissue culture were from GIBCO BRL (Auckland, NZ) and RPMI 1640 medium was frp, Euroclone (Milano, Italy). 1,2-dioleoyl-*sn*-glycero-3-phosphoethanolamine (DOPE), L-α-phosphatidylethanolamine-N-(lissamine rhodamine B sulfonyl) (RhPE) and L-α-phosphatidylcholine (PC) were from Avanti Polar Lipids (Alabaster, AL, USA); cholesteryl hemisuccinate (CHEMS) and cholesterol (Chol) were from Sigma. ER-tracker blue-white DPX, cholera toxin subunit B (CTB)-Alexa Fluor 594 conjugate (CTB-594), CTB-Alexa Fluor 488 conjugate (CTB-488), transferrin-Alexa Fluor 594 conjugate (Tf-594), dextran-Alexa Fluor 594 (Dex-594), Organelle Lights ER-OFP (ER-OFP), MitoTracker Red CMXRos and LysoTracker Red DND-99 were from Invitrogen (Eugene, OR, USA).

Cell culture

MDBK (Madine Darbin bovine kidney), HeLa and HUH7 cells were cultivated in tissue culture flasks at 37°C and 5% CO_2 in RPMI 1640 medium supplemented with L-glutamine (2 mM), 10% (v/v) heat-inactivated foetal bovine serum, penicillin (50 U/ml) and streptomycin (50 μg/ml). The number of passages varied between four and ten for all cell lines tested.

Preparation of liposomes

For pH-sensitive liposomes, DOPE and CHEMS lipid solutions were mixed in a molar ratio of 3 : 2, placed into round-bottom flask and the chloroform was removed by rotary evaporation (Laborota 4000, Heidolph Instruments GmbH & Co. KG, Schwabach, Germany) under reduced pressure for 1–2 hrs. The dry lipid film was hydrated in PBS to yield a final concentration of 10 mmol of lipids per litre. Liposome membrane was labelled with 0.5 mol% RhPE. For liposomes-containing calcein the lipid film was hydrated in a 50 mM calcein solution in PBS. The liposomes solutions were sonicated for 1.5 hrs with a bath sonicator, and the liposomes were extruded 21 times through a polycarbonate filter of 100-nm pore diameter (Nucleopore, Whatman, Clifton, NJ, USA), using a Mini-Extruder device (Avanti Polar Lipids). The non-encapsulated calcein was removed by gel-filtration chromatography on a 10 × 20 Sepharose CL-4B column (Amersham Biosciences, Fairfield, CT, USA). In some experiments calcein was replaced by lactoferrin protein. Bovine lactoferrin (Morinaga Milk Industry, Zamashi, Japan) was labelled with Texas Red-X succinimidyl ester (Molecular Probes, Eugene, OR, USA) according to the manufacturers protocol. The unbound dye was removed by gel-chromatography on Sephadex G-25. The labelled protein (LF-Tx) was included in DOPE : CHEMS liposomes as above. pH-insensitive liposomes were made of PC : Chol (3 : 1 molar ratio) by the same procedure as pH-sensitive liposomes.

Drug treatments

Cells were pre-incubated for 30–60 min. at 37°C in medium containing 200 nM bafilomycin A1 (BAF), 30 μM nocodazole (NOCO), 10 μM cytochalasin D (CYTD), 10 mM methyl-β-cyclodextrin (MβCD), 50 μg/ml nystatin (NYST), 0.2 mM dansylcadaverine (DC), 10 μg/ml chlorpromazine (CP), 5 μg/ml Brefeldin A (BFA) or 50 mM NH_4Cl. The drugs were present during the liposome treatment and maintained throughout the chase period.

Transduction experiments with the ER-OFP

The ER-OFP construct cloned into a baculovirus encodes the orange fluorescent protein fused with the ER signal sequence of calreticulin and the KDEL retention sequence to allow ER localization. Cells were seeded on chamber slides 1 day prior to transduction experiments and allowed to reach 60–80% confluence before proceeding with the treatment with the ER-OFP reagents according to the manufacturers' protocol. After 24 hrs the cells were incubated for 30 min. with liposome-included calcein, washed and chased 5 hrs at 37 °C before imaging.

Fluorescence microscopy techniques

DOPE : CHEMS liposomes encapsulating calcein and/or DOPE : CHEMS liposomes containing RhPE in their membrane were added to the cells grown on chamber slides (Nunc, Roskilde, Denmark) at final concentration of ~0.1 mM. Cells were incubated with liposomes for 30 min. at 37°C, or 1 hr at 4°C, washed with culture medium and visualized on a Nikon Eclipse E600 fluorescence microscope (Tokyo, Japan) at different chase times. ER-tracker (1 μM), Dex-594 (0.1–1 mg/ml), CTB-594 or CTB-488 (5 μg/ml) were used for intracellular co-localization of liposomes. To visualize the endocytic pathway HeLa cells labelled with calcein liposomes were treated for 15 min. with Tf-594 (50 μg/ml), followed by 15 min. incubation in the absence of the dye.

All the experiments were performed with live cells with the exception of laser scanning confocal microscopy. In this latter case HeLa cells were treated with liposome-included calcein and CTB-594 for 30 min. (37°C), washed and chased for 5 hrs. Cells were fixed for 15 min. with 4% paraformaldehyde (PFA) and visualized with a Nikon TE2000 microscope equipped with an Ar 488 laser, a He-Ne 543 laser, a diode laser at 408 nm and a 60× oil immersion objective (N.A. 1.49 Plan Apo TIRF). Sequential scanning of 0.2-μm sections was used for co-localization studies. A total of 61 images were captured using Nikon EZ-C1 software and analysed using either Nikon EZ-C1 viewer or NIH ImageJ software. Three-dimensional blind deconvolution was made with Autoquant software. All the images shown are representative of at least two independent experiments.

FACS analysis

MDBK or HUH7 cells were seeded in six-well plates 1 day prior to experiment and allowed to reach ~70–80% confluence. Cells were pre-treated or not with different inhibitors (30 min., 37°C) and liposomes-containing calcein were added for 30 min. at 37°C. Cells were washed and incubated for 1.5 hrs in fresh medium to allow the calcein release from liposomes. The drugs were present during the chase period. Cells were detached with trypsin ethylenediaminetetraacetic acid, suspended in FACS buffer (2% foetal bovine serum in PBS), and subjected to FACS analysis. FACS analysis were performed with a FACSCalibur (BD Biosciences, Bedford, MA, USA) equipped with a 488 nm argon ion laser. Fluorescence emission of samples (10,000 events/sample) was collected at 530 nm (FL1) on a logarithmic scale with a 1024 channel resolution. The analysis gate was set on live cells, and the median fluorescence intensity (MFI) was determined using CellQuest Pro software (BD Biosciences). Statistical data was represented from the MFI of three independent experiments.

Results

Accumulation of liposome-delivered cargo within a perinuclear organelle

To follow the intracellular trafficking of internalized vesicles, we used liposomes loaded with the membrane-impermeant calcein molecule [16] and liposomes labelled with the lipophilic marker RhPE. MDBK cells were pulsed with equal amounts of both liposomes for 30 min. and chased for 5 hrs at 37°C. RhPE liposomes were slowly internalized in vesicular structures found mainly near the plasma membrane (Fig. 1A). Starting 2 hrs from internalization, most of the liposomal lipids and calcein accumulated around the nuclei, showing a partial overlapping with the ER-tracker, a cell-permeant dye, highly selective for the ER [17]. Although the ER-tracker stained both perinuclear and peripheral ER, confirming previous reports [18], calcein and RhPE fluorescence were confined to the perinuclear area. Further confirmation for the ER localization of calcein came from its overlapping with another ER marker, the orange fluorescent protein KDEL (Fig. 1D). This was a surprising finding, because these types of liposomes that destabilize at acidic pH have been reported to deliver their content mainly to the cytoplasm [19, 20]. In contrast, free calcein and pH-insensitive liposomes made of PC : Chol were inefficiently internalized (Fig. 1B and C). Moreover, the calcein cargo did not overlap with the Golgi, lysosomes or mitochondria markers tested (Fig. S1). Similarly, liposome-treated HeLa cells showed a prominent overlapping of calcein with the two ER markers suggesting that this maybe a more common intracellular traffic route (Fig. 3).

Internalization of liposome cargo is affected by cholesterol depletion and endocytosis inhibitors

Using various inhibitors of endocytosis we examined the liposomes uptake into the cell. The effects of these drugs were examined by testing the uptake of specific endocytosis markers (dextran, transferrin and lactosylceramide) in mock *versus* treated cells (Fig. S2). Because several reports have documented the role of cholesterol in the endocytic pathway, we performed cholesterol depletion with MβCD or sequestration of plasma membrane cholesterol with NYST to block the cholesterol-dependent internalization routes [15, 21–23]. As shown by FACS analysis MβCD inhibitor produced a 99% loss of calcein fluorescence in liposomes treated cells, whereas NYST resulted in a ~61% decrease in fluorescence (Fig. 2A and B).

To test the role of actin fibres we used CYTD, an inhibitor of actin polymerization [24, 25]. Treatment of cells with CYTD had relatively little influence on the liposomal entry, as shown by FACS measurements (Fig. 2A and B).

To determine if the liposomes were internalized by the cells through a clathrin-mediated pathway we tested the effects of CP and DC, inhibitors of clathrin-mediated coated vesicle formation [26–30]. Only 22–25% of the control cells fluorescence remained in the DC and CP treated cells (Fig. 2B). The results indicated that the liposomes uptake was inhibited by cholesterol depletion while being dependent on clathrin-mediated processes.

To investigate whether intact microtubules were required for internalization we have used NOCO which significantly reduced the initial liposome uptake to 65% of the control, indicating a role for microtubules in this process (Fig. 2A and B).

Because the uptake into caveosomes is pH independent we next investigated whether the liposomal transport was affected by pH changes [31]. First, BAF, which inhibits endosomes acidification by specifically blocking the endosomal ATPase pumps, has been evaluated [32]. As shown in Fig. 2A, the fluorescence intensity measured by FACS indicated a dramatic loss which went up to 80% from the fluorescence of the untreated cells (Fig. 2B). On the other hand, treatment of cells with NH_4Cl to elevate the endosomal pH [33], reduced the cell fluorescence to approximately 35% of the positive control (Fig. 2A and B). The uptake process involved a prominent pathway which does not require actin, and is dependent on microtubule transport (65%), but also on endosome acidification (65–80%).

Microtubule and pH-dependent trafficking of liposome cargo

We further visualized the fluorescence distribution of the liposome cargo in cells treated with the above inhibitors for 5 hrs (Fig. 2C). Treatment of cells with CYTD led to a major cell shape modification due to the actin fibre de-polymerization with a diffuse distribution of calcein within the cell. MβCD had dramatically impaired liposomes entry; hence calcein fluorescence was almost absent. Diffuse fluorescence with some vacuolar structures was observed in cells treated with NYST, DC, CP and NH_4Cl. In BAF-treated cells the calcein fluorescence was vague and localized in the vicinity of the plasma membrane, with no co-localization with the ER-tracker (Fig. 2D). Disruption of the microtubule cytoskeleton with NOCO resulted in a rather faint punctuate calcein pattern different from

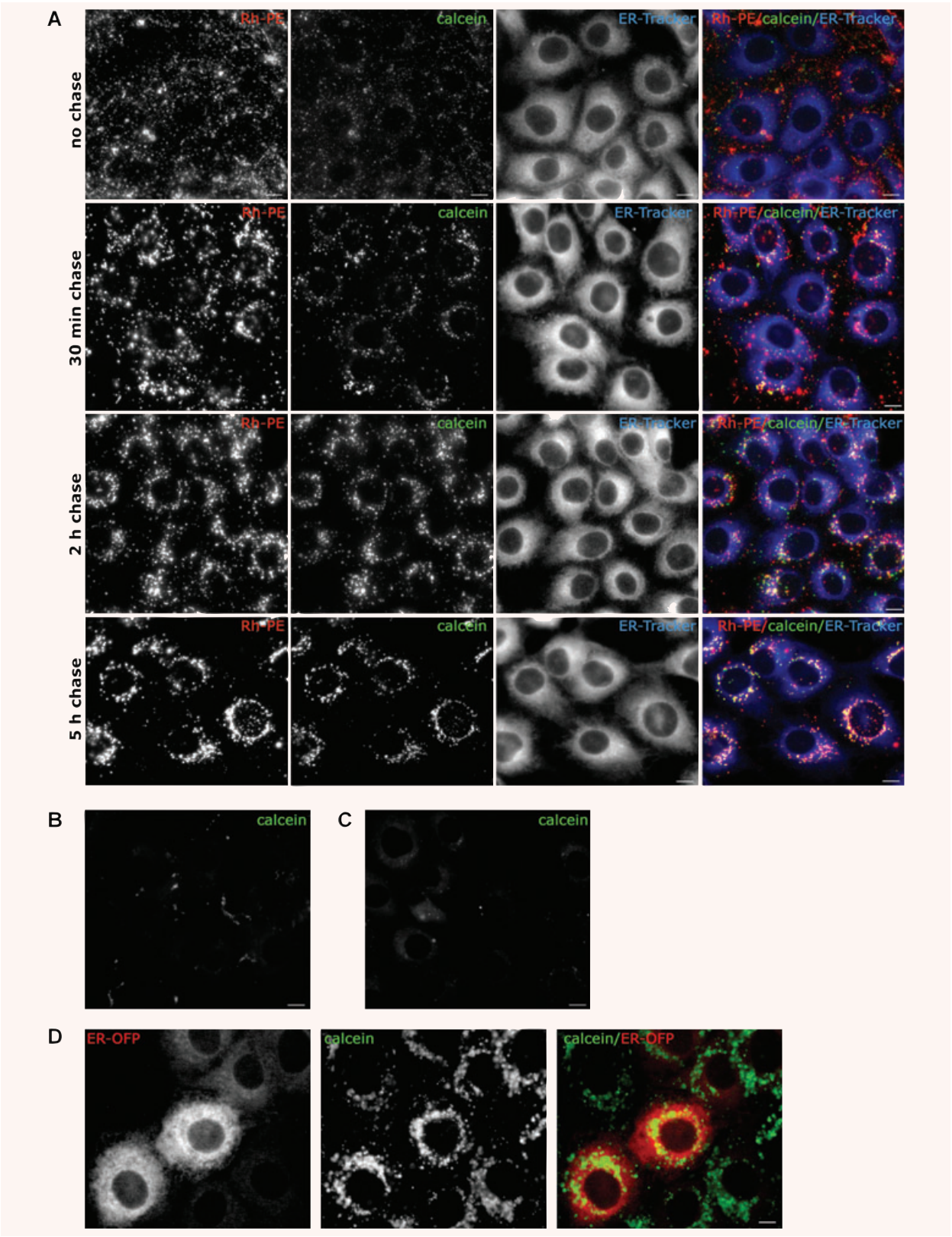

Fig. 1 Internalization of vesicles-containing calcein results in calcein accumulation within the ER. MDBK cells were incubated with liposome-loaded calcein and RhPE liposomes for 30 min. at 37°C, washed, and kept in culture for the indicated times. (**A**) 30 min. before visualization cells were incubated with the ER marker, ER-tracker (*blue*). Lipid marker RhPE and calcein were visualized in *red* and *green* channel, respectively. (**B**) Cells were treated for 30 min. at 37°C with ~0.2 mM PC : Chol liposomes-included calcein, washed and chased 2 hrs in fresh medium. (**C**) Cells were treated with free calcein for 30 min. at 37°C, washed and incubated for 2.5 hrs in fresh medium. (**D**) MDBK cells transduced with ER-OFP (*red*) were incubated with liposome-included calcein for 30 min. at 37°C and imaged after 5 hrs chase. Scale bar 10 μm.

the bright fluorescent staining of the perinuclear region in control cells (Fig. 2D). These experiments show that the perinuclear accumulation of the cargo is impaired by the endosomes alkalinisation and requires an intact microtubular network.

Calcein and lactoferrin co-localize with CTB in the ER of HeLa cells

To further investigate the intracellular localization of liposome cargo, we used fluorescently labelled human transferrin as endosomal marker, fluorescent dextran as lysosomal marker and CTB as marker for ER. Previous work has reported that transferrin receptor reached recycling endosomes 30 min. after internalization [34]. In our experiment, HeLa cells were treated for 30 min. with liposomes-containing calcein, washed and incubated with liposome-free medium for 3 hrs and Tf-594 was added 30 min. before visualization. As seen in Fig. 3B, calcein and transferrin had different distribution patterns.

Cholera toxin enters the cells mainly through a caveolae-mediated pathway and is internalized within caveosomes which transport it to the Golgi compartment [13, 35]. From here the toxin takes the retrograde pathway reaching the ER in about 3 hrs [36]. As MDBK cells did not internalize the CTB we used HeLa cells which have efficiently uptaken the toxin. We have treated the cells with both the calcein liposomes and the CTB, followed by visualization after 3–5 hrs of chase by conventional microscopy. As seen in Fig. 4C, the distributions of CTB (red) and calcein (green) were very similar, indicating that a significant percentage of calcein reaches the ER of these cells. We also performed co-localization experiments with liposome-loaded calcein and CTB after 5 hrs internalization in fixed HeLa cells. A total of 61 Z-stack images were acquired using a confocal microscope and the 3D deconvolution was made with Autoquant software. As seen in Fig. 3D, although a proportion of the calcein fluorescence has been lost after fixation procedure, the remaining calcein co-localized with CTB in the ER. Further, calcein was shown to substantially overlap with the orange fluorescent protein-KDEL, confirming its ER localization found in the presence of the ER-tracker and cholera toxin (Fig. 3E).

To test whether the liposomes trafficking involved the Golgi apparatus we used liposomes containing Texas Red-labelled lactoferrin (LLF-Tx) and CTB-Alexa Fluor 488 (CTB-488) in the presence of BFA which is known to block the retrograde transport of the cholera toxin [30]. As seen in Fig. 4, LLF-Tx and CTB-488 co-localized in HeLa cells at 5 hrs after internalization. In contrast, when cells were treated with BFA, only lactoferrin displayed perinuclear localization, whereas CTB was predominantly spread at the cell periphery.

Further confirmation for the lack of Golgi involvement in the plasma membrane-to-ER transport of lipid vesicles came from the lack of co-localization of either calcein or RhPE with NBD C_6-ceramide/ TR C_5-ceramide, which are well-characterized Golgi markers (Fig. S1A and B). No significant co-localization of loaded calcein with lysosomes (Fig. S1C and D) and mitochondria (Fig. S1E) could be observed.

Vesicular trafficking is not impaired in caveolin-1-deficient cells

To estimate the role of caveolin-dependent endocytosis for the pH-sensitive liposomes trafficking, we have analysed their uptake by HUH7, a human hepatoma cell line with no detectable levels of caveolin-1 [15]. As shown in Fig. 5A, even in the absence of caveolin-1, HUH7 internalized the pH-sensitive liposomes and both calcein and RhPE-labelled lipids were superimposed with the ER-tracker at 3–5 hrs after internalization. Only scarce overlapping with Tf-594 (Fig. 5B) and Dex-594 (Fig. 5C) was observed in HUH7 cells. Next, we have used the endocytosis inhibitors to measure the liposomal uptake by HUH7 cells by flow cytometry (Fig. 5D and E). In an experiment similar with the one in Fig. 2B, BAF and NH_4Cl reduced the uptake by 65–70%, whereas CP and DC inhibition varied between 35% and 65%. NOCO showed only 46% inhibition and CYTD went up to 80%. Depletion of membrane cholesterol by MβCD had the most powerful inhibitory effect (more than 90% inhibition). NYST treatment resulted in a 78% inhibition of the liposome uptake in HUH7 cells. We conclude that cholesterol depletion strongly inhibits the liposome uptake in these cells deficient in caveolin-1, as previously reported for the SV40 entry in HUH7 cells [15]. In contrast to SV40, liposomes require microtubules for entry, indicating that the uptake pathway maybe different. In addition, non-caveolae non-clathrin endocytosis could account for 40–65% of the pathways, whereas the rest is clathrin mediated.

Discussion

Internalized cargo can escape the endocytic pathway to reach the ER by either direct or retrograde pathways. Direct pathways may

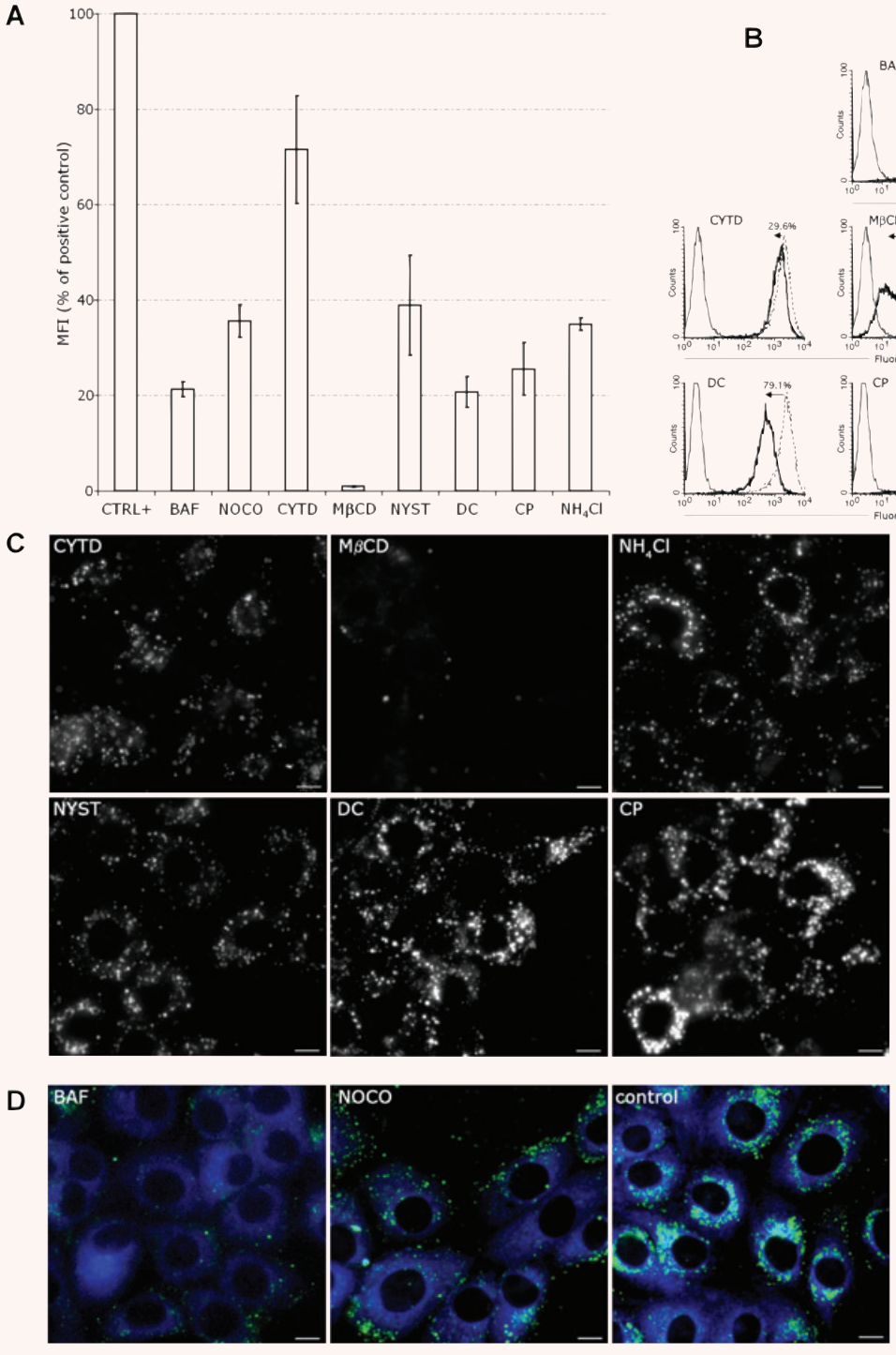

Fig. 2 Effects of inhibitors on the liposomes uptake and traffic. (**A** and **B**) Flow cytometry for the analysis of liposome uptake in the presence or absence of inhibitors (*black line* and *dotted line histograms*, respectively). Cells were treated or not with inhibitors and liposomes-containing calcein were added as in 'Materials and methods'. *Grey line histograms* represent negative control cells. (**A**) Median fluorescence intensity of calcein in positive control cells = 100%. Error bars indicate standard deviation ($n = 3$ independent experiments). (**B**) The numbers in the histogram plots were calculated from the median fluorescence and indicate the percentage of uptake inhibition induced by drugs. Median fluorescence of positive control cells was set to 100%. (**C**) After 1 hr pre-treatment with inhibitors MDBK cells were incubated with liposome-included calcein for 30 min. at 37°C in the presence of drugs. Liposomes were removed and cells were further incubated in the presence of drugs for either 2 hrs (CYTD), or 5 hrs (the other inhibitors). (**D**) As in (**C**), but 30 min. before visualization cells were incubated with the ER marker, ER-tracker (*blue*). Scale bar 10 μm.

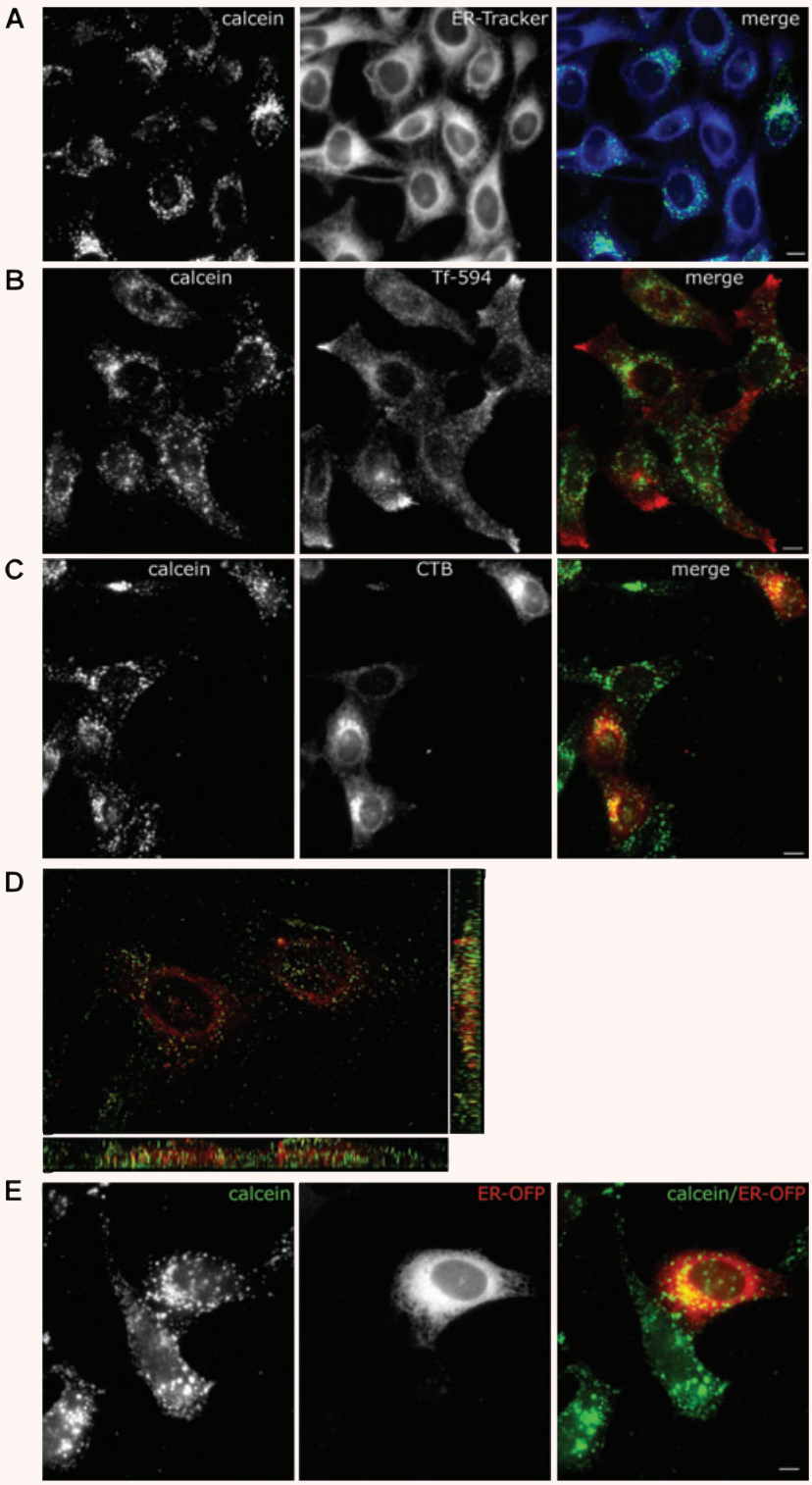

Fig. 3 Co-localization of calcein with CTB in the ER of HeLa cells. (**A**) HeLa cells were treated with liposome-loaded calcein (30 min., 37°C), and chased for 3 hrs in fresh medium. 30 min. before visualization cells were labelled with ER-tracker. Live cells were visualized with Nikon E600 microscope. (**B**) As in (**A**), except that Tf-594 were added at the end of the chase for 15 min., washed away and the cells were further incubated for another 15 min. (**C**) CTB and liposome-included calcein were allowed to enter HeLa cells for 30 min. at 37°C. Cells were washed and incubated in medium for 3 hrs. (**D**) Confocal image of HeLa cells treated as in (**C**) except that after 5 hrs of chase the sample was fixed with 4% PFA. (**E**) HeLa cells transduced with ER-OFP (*red*) were incubated with liposome-included calcein (30 min., 37°C) and imaged after 5 hrs chase. Scale bar 10 μm.

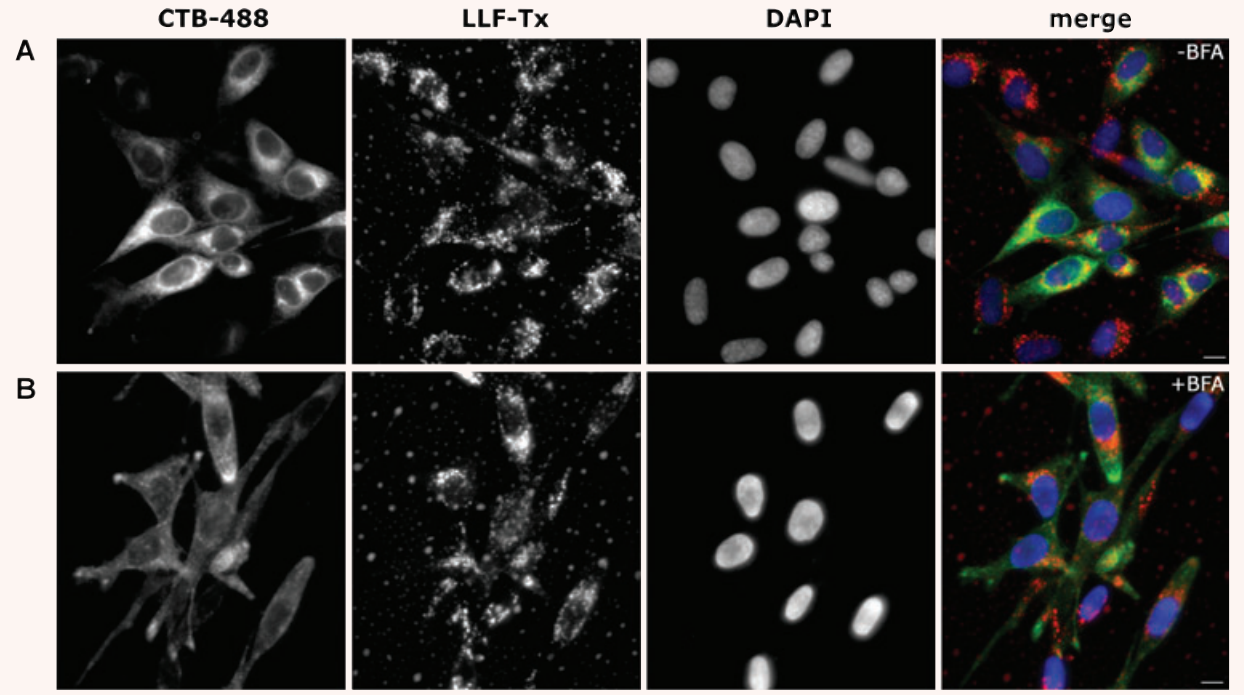

Fig. 4 Lipid vesicles with lactoferrin do not use the retrograde pathway to reach the ER. HeLa cells were not treated (**A**) or pre-treated for 30 min. with BFA (**B**), and liposome-loaded LF-Tx (LLF-Tx), and CTB-Alexa Fluor 488 conjugate (CTB-488) were added to the cells for 30 min. The cells were washed and chased for 5 hrs in the presence (**B**) or absence (**A**) of the inhibitor. The cell nuclei were labelled with DAPI. Scale bar 10 μm.

involve activated caveosome routes, as in the case of some viruses [14, 15], or may use constitutive endocytic pathways, as shown here for extracellular lipid vesicles. A likely scenario based on our results is that a lipid vesicle is able to bypass the degradative cytoplasmic pathways by triggering constitutive ER targeting routes upon entry.

To investigate the internalization of an extracellular lipid vesicle we made use of PE-based fusogenic liposomes with ubiquitous uptake in mammalian cells. Using two tumour-derived cell lines (HeLa and HUH7) and a normal, non-transformed one (MDBK) we found that multiple routes were used by these vesicles to penetrate the cells. However, regardless of delivery route, all cells had in common a progressive perinuclear accumulation of the cargo and lipids. This was dependent upon endosomal acidification and availability of microtubule pathways. The perinuclear clustering was paralleled by a time-dependent dilution de-quenching of calcein cargo as a result of its release from liposomes. Liposome destabilization and fusion with the endosome bilayer upon endosomal acidification has been previously documented [16]. Basically, the acidic environment can induce the formation of non-bilayer phase in the DOPE : CHEMS liposome, facilitating the fusion by lipid rearrangements between the two membranes. Whether this fusion is followed or not by release of the encapsulated material into the cytosol, is still a matter of debate [37–39]. Our data clearly indicate that the mechanism of the intracellular delivery is more complicated that initially thought with little indication for vesicle leakage into the cytoplasm. Noteworthy, the fusion of destabilized liposomes with the endosomal membrane does not necessarily involve destabilization of the endosomes, as it has been repeatedly suggested [40–42]. This is in contrast with many viruses pathways, which upon fusion with the endosomal membrane are released into the cytosol. Bovine diarrhoea virus, for example, a virus infecting MDBK cells, is endocytosed by clathrin coated vesicles [43, 44], in a cholesterol-dependent manner, similar to the fusogenic liposomes entry. In this case, it is highly likely that besides the fusion of the viral membrane with the endosome, the low pH triggers additional events (related to either generation of pores or endosome destabilization) leading to the cytoplasmic delivery of the viral RNA. Similarly, influenza virus is translocated in the cytoplasm at acidic pH of the early endosomes. Initially designed as virus mimics liposomes start to reveal some of the molecular events required for efficient virus infection. Further confirmation comes from the reported cytoplasmic delivery of a liposome preparation modified with a pH-sensitive fusogenic peptide [45]. This would be in accordance with our findings supporting a mechanism based on the transient formation of liposome-endosome organelles following an ER delivery pathway. We documented the ER targeting based on the partial co-localization of the liposomal cargo (calcein and lactoferrin) with several ER markers: ER-tracker, cholera toxin and an ER targeted fluorescent

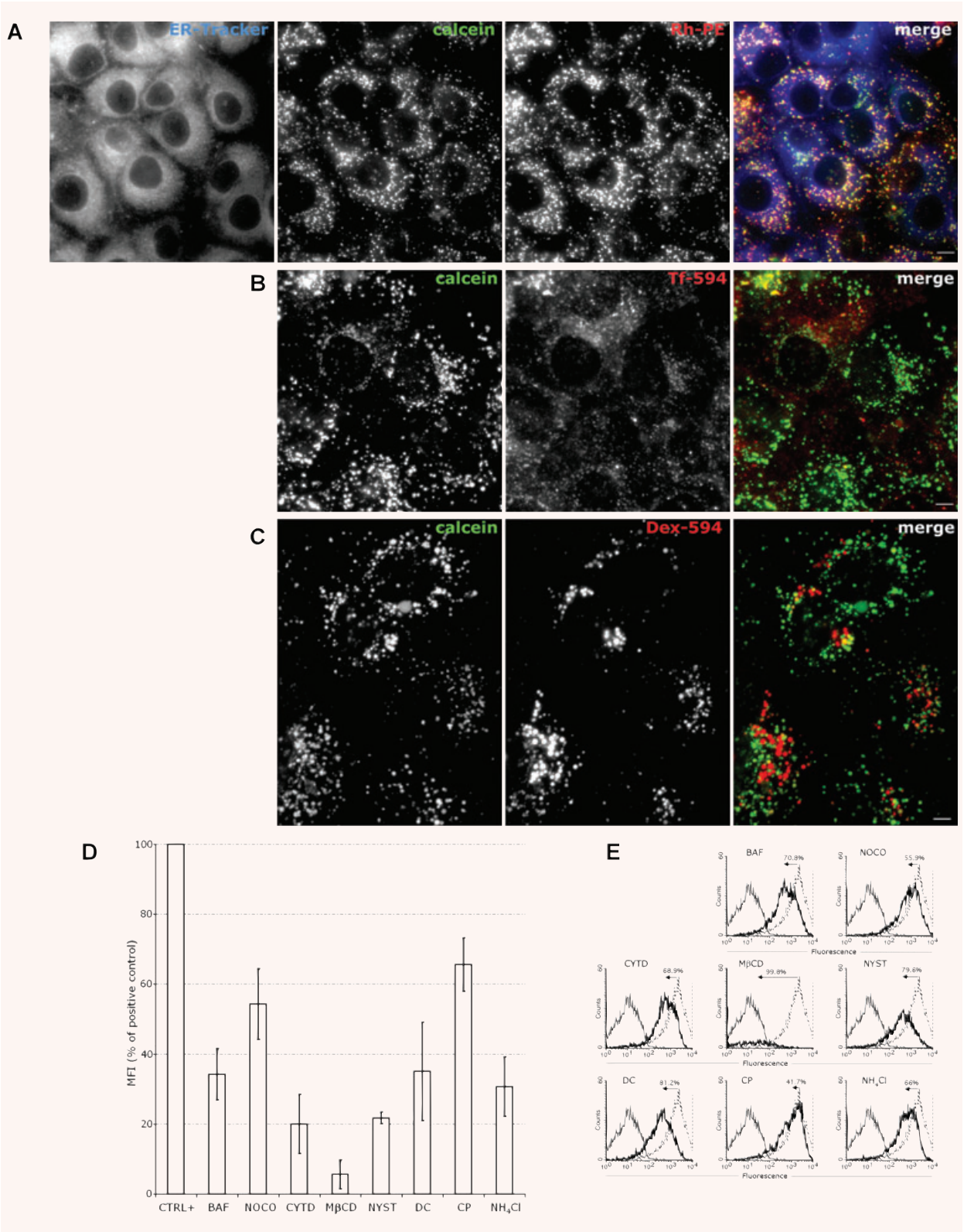

Fig. 5 Endocytosis of liposomes-containing calcein in HUH7 cells. (**A**) HUH7 cells were incubated with liposome-loaded calcein and RhPE liposomes for 30 min. at 37°C, washed and cultivated for 5 hrs. 30 min. before visualization cells were labelled with ER-tracker. (**B**) HUH7 cells were incubated for 30 min. with liposome-entrapped calcein, washed, and cultivated in liposome-free medium for ~4 hrs. 30 min. before visualization cells were labelled with Tf-594. (**C**) Cells were treated as in (**B**), except that the Dex-594 was added 48 hrs before the liposome-loaded calcein. Scale bar 10 μm. (**D** and **E**) Flow cytometry for the analysis of liposome uptake in the presence or absence of inhibitors (*black line* and *dotted line histograms*, respectively). HUH7 cells were treated or not with inhibitors and liposomes-containing calcein were added as in 'Materials and methods'. *Grey line histograms* represent negative control cells. (**D**) Median fluorescence intensity of calcein in positive control cells = 100%. Error bars indicate standard deviation ($n = 3$ independent experiments). (**E**) The numbers in the histogram plots were calculated from the median fluorescence and indicate the percentage of uptake inhibition induced by drugs. Median fluorescence of positive control cells was set to 100%.

protein. Besides this pathway one cannot exclude other routes such as lysosomal or cytoplasmic, which may be favoured by subtle variations in the lipid composition of the fusogenic vesicles.

Previous reports have shown that PE-based liposomes enter the cells using multiple pathways [39]. We found that PE-based fusogenic liposomes entered MDBK cells predominantly by clathrin-dependent endocytosis. Caveolae-deficient cells line, such as HUH7, internalized the lipid vesicles not only by clathrin mediated but also by non-clathrin non-caveolae pathways.

Although different endocytic pathways were predominant in the cell lines tested, we found a ubiquitous requirement for cholesterol-mediated internalization route. This was effective in both caveolin-1^+ and caveolin-1^- cells because MDBK and HUH7 cells displayed an impaired uptake of liposomal calcein under cholesterol depletion, supporting the notion that caveolin absence does not impair the plasma membrane-ER trafficking, despite noticeable differences between the two intracellular routes. Endocytosis to caveosomes is blocked by cholesterol depletion, although this treatment is not highly specific [31, 46]. Indeed, it has been reported that cholesterol depletion can inhibit clathrin coated pit budding [47–49]. As HUH7 cells are deficient in caveolin-1, and the uptake of lipid vesicles is predominantly clathrin independent, it is possible that cholesterol depletion may also affect other endocytosis pathways [50, 51]. GPI-enriched endosomal compartment (GEEC) pathway is another possible route of liposome internalization [52]. Interestingly, actin polymerization is required both for this pathway and for liposomes uptake in the HUH7 cells. Hence, GEEC pathway could remain a possible way of liposomal uptake in cell lines.

In an attempt to characterize the destination organelle of the encapsulated cargo by preserving intact the subcellular structures we constantly avoided the use of cell fixation, reported to induce artefacts [53]. This might have been an important issue explaining why this particular ER targeting pathway has not been found before, despite the intense scrutiny of the liposome delivery routes. This route may find significant applications in the drug targeting of ER processes such as protein aggregation and glycosylation. Indeed, it has been recently shown that glycosylation inhibitors could be efficiently delivered to the ER of various cells such as melanoma and HIV infected T cell when encapsulated in the DOPE : CHEMS liposomes [54, 55].

The microtubule-dependent endocytic transport to the ER indicated two alternative pathways: (*i*) cargo is transported from the early endosomes to late endosomes, a route known to require microtubules and from here to the TGN and further to the ER, by the retrograde pathway; (*ii*) cargo is directly transported from fused endosomes to the ER, a pathway that has not been consistently documented so far. To discriminate between these two pathways, we used Golgi markers in co-localization studies and BFA to impair the TGN-to-ER traffic. Besides the absence of cargo co-localization with the Golgi we found that in HeLa cells BFA had no effect on the intracellular trafficking of encapsulated lactoferrin. In contrast, CTB remained in pre-Golgi structures with no co-localization with the ER, indicating that there is a different direct pathway taken by the liposomal cargo en route to the ER.

In conclusion, lipid vesicles are internalized by both clathrin-mediated and clathrin-independent endocytosis pathways which require an acidification step for liposomes destabilization and fusion with the endosomes. The fusion event possibly triggers a microtubule driven pathway which avoids classical sorting endosomes and favours an ER pathway. This is an alternate to the SV40 virus caveolar route using a pH dependent, direct plasma membrane-to-ER pathway to efficiently deliver extracellular encapsulated cargo to the ER. Although further studies are needed to dissect this novel pathway in more detail, the finding of a second major ER targeting route leads to the idea that the import of molecules from the outside cell into the ER could be as important for the cell function as its secretion processes. On the other hand, our findings add to the extensive use of liposomes as drug delivery carriers, by proposing this new ER delivery route. This pathway may be used to specifically deliver to the ER drugs such as chemical chaperones, glycosylation inhibitors, cholesterol synthesis inhibitors, anti-ER stress drugs.

Acknowledgements

We thank Professor Raymond Dwek for his constant support and useful discussions and for critically reading the manuscript. This work was partially supported by a grant for SMP from the University of Oxford.

Supporting Information

Additional Supporting Information may be found in the online version of this article.

Fig. S1 The calcein cargo does not co-localize with the Golgi, lysosomes or mitochondria markers. MDBK cells were incubated for 30 min. with RhPE liposome or with liposome-included calcein. The Golgi compartment was labelled with (**A**) NBD C_6-ceramide (*green*), or (**B**) TR C_5-ceramide (*red*). The acidic compartment was labelled with LysoTracker Red (**C**), or with dextran-Alexa Fluor 594 (**D**), the mitochondrion with MitoTracker Red (**E**) and the ER with ER-OFP (**F**).The cells were visualized after 3–5 hrs. Note that the red channel signal was increased to emphasize the LysoTracker fluorescence. No significant co-localization with Golgi apparatus, lysosomes and mitochondria could be observed. Note the substantial overlapping with the ER marker. Scale bar 10 μm.

Fig. S2 Uptake of dextran, lactosylceramide and transferrin in cells treated with endocytosis inhibitors. (**A**) HeLa cells were mock treated or pre-incubated with BAF (200 nM) or NOCO (30 μM) for 30 min., followed by the uptake of the dextran-Alexa Fluor 488 (Dex-488) (1 mg/ml) for 25 min. at 37°C (**B**) MDBK cells were pre-treated or not (mock) with MβCD (10 mM) or NYST (50 μg/ml) for 30 min., incubated with BODIPY FL C_5-lactosylceramide (LacCer) 30 min. at 10°C, washed and chased 10 min. at 37°C. We determined the ability of the lactosylceramide to penetrate the treated cells, because this compound uptake through the caveolar pathway is blocked by sterol-binding compounds [23]. (**C**) As in (**A**), but instead of Dex-488 the uptake of Tf-594 (50 μg/ml) as marker for clathrin-mediated endocytosis was observed. Cells were pre-treated with DC (0.2 mM), CP (10 μg/ml), NH4Cl (50 mM), or CYTD (10 μM).Cells were washed, fixed with PFA 4%, mounted with VectaShield with DAPI and imaged. All inhibitors yielded more diffuse fluorescence of the markers as compared with the mock cells, demonstrating the specificity of these drugs for the endocytic pathways analysed.

This material is available as part of the online article from: http://www.blackwell-synergy.com/doi/abs/10.1111/j.1582-4934.2009.00724.x
(This link will take you to the article abstract).

Please note: Wiley-Blackwell are not responsible for the content or functionality of any supporting materials supplied by the authors. Any queries (other than missing material) should be directed to the corresponding author for the article.

References

1. **Sevier CS, Qu H, Heldman N, *et al.*** Modulation of cellular disulfide-bond formation and the ER redox environment by feedback regulation of Ero1. *Cell*. 2007; 129: 333–44.
2. **Frand AR, Cuozzo JW, Kaiser CA.** Pathways for protein disulphide bond formation. *Trends Cell Biol*. 2000; 10: 203–10.
3. **Anelli T, Sitia R.** Protein quality control in the early secretory pathway. *EMBO J*. 2008; 27: 315–27.
4. **Ellgaard L, Molinari M, Helenius A.** Setting the standards: quality control in the secretory pathway. *Science*. 1999; 286: 1882–8.
5. **Lipson KL, Ghosh R, Urano F.** The role of IRE1α in the degradation of insulin mRNA in pancreatic β-cells. *PLoS ONE*. 2008; 3: e1648.
6. **Hoyer-Hansen M, Jaattela M**. Connecting endoplasmic reticulum stress to autophagy by unfolded protein response and calcium. *Cell Death Differ*. 2007; 9: 1576–82.
7. **Robinet P, Fradagrada A, Monier MN, *et al.*** Dynamin is involved in endolysosomal cholesterol delivery to the endoplasmic reticulum: role in cholesterol homeostasis. *Traffic*. 2006; 7: 811–23.
8. **Gagnon E, Duclos S, Rondeau C, *et al.*** Endoplasmic reticulum-mediated phagocytosis is a mechanism of entry into macrophages. *Cell*. 2002; 110: 119–31.
9. **Fevrier B, Raposo G.** Exosomes: endosomal-derived vesicles shipping extracellular messages. *Curr Opin Cell Biol*. 2004; 16: 415–21.
10. **Vincent-Schneider H, Stumptner-Cuvelette P, Lankar D, *et al.*** Exosomes bearing HLA-DR1 molecules need dendritic cells to efficiently stimulate specific T cells. *Int Immunol*. 2002; 14: 713–22.
11. **Wolfers J, Lozier A, Raposo G, *et al.*** Tumor-derived exosomes are a source of shared tumor rejection antigens for CTL cross-priming. *Nat Med*. 2001; 7: 297–303.
12. **Hearing VJ.** Regulating melanosomes transfer: who's driving the bus? *Pigment Cell Res*. 2007; 20: 334–5.
13. **Fujinaga Y, Wolf AA, Rodighiero C, *et al.*** Gangliosides that associate with lipid rafts mediate transport of cholera and related toxins from the plasma membrane to endoplasmic reticulum. *Mol Biol Cell*. 2003; 14: 4783–93.
14. **Lilley BN, Gilbert JM, Ploegh HL, *et al.*** Murine polyomavirus requires the endoplasmic reticulum protein Derlin-2 to initiate infection. *J Virol*. 2006; 80: 8739–44.
15. **Damm EM, Pelkmans L, Kartenbeck J, *et al.*** Clathrin- and caveolin-1-independent endocytosis: entry of simian virus 40 into cells devoid of caveolae. *J Cell Biol*. 2005; 168: 477–88.
16. **Simoes S, Slepushkin V, Duzgunes N, *et al.*** On the mechanism of internalization and intracellular delivery mediated by pH-sensitive liposomes. *Biochim Biophys Acta*. 2001; 1515: 23–37.
17. **Xu L, Harada H, Yokohama-Tamaki T, *et al.*** Reuptake of extracellular amelogenin by dental epithelial cells results in increased levels of amelogenin mRNA through enhanced mRNA stabilization. *J Biol Chem*. 2006; 281: 2257–62.
18. **Ong HL, Liu X, Tsaneva-Atanasova K, *et al.*** Relocalization of STIM1 for activation of store-operated Ca^{2+} entry is determined by the depletion of subplasma membrane endoplasmic reticulum Ca^{2+} store. *J Biol Chem*. 2007; 282: 12176–85.
19. **Straubinger RM, Düzgünes N, Papahadjopoulos D.** pH-sensitive liposomes mediate cytoplasmic delivery of encapsulated macromolecules. *FEBS Lett*. 1985; 179: 148–54.
20. **Van Bambeke F, Kerkhofs A, Schanck A, *et al.*** Biophysical studies and intracellular destabilization of pH-sensitive liposomes. *Lipids*. 2000; 35: 213–23.
21. **Le PU, Nabi IR.** Distinct caveolae-mediated endocytic pathways target the Golgi apparatus and the endoplasmic reticulum. *J Cell Sci*. 2003; 116: 1059–71.
22. **Bousarghin L, Touze A, Sizaret PY, *et al.*** Human papillomavirus types 16, 31, and

58 use different endocytosis pathways to enter cells. *J Virol*. 2003; 77: 3846–50.

23. **Sharma DK, Brown JC, Choudhury A, *et al.*** Selective stimulation of caveolar endocytosis by glycosphingolipids and cholesterol. *Mol Biol Cell*. 2004; 15: 3114–22.
24. **Misinzo G, Meerts P, Bublot M, *et al.*** Binding and entry characteristics of porcine circovirus 2 in cells of the porcine monocytic line 3D4/31. *J Gen Virol*. 2005; 86: 2057–68.
25. **Cuadras MA, Arias CF, Lopez S.** Rotaviruses induce an early membrane permeabilization of MA104 cells and do not require a low intracellular Ca2+ concentration to initiate their replication cycle. *J Virol*. 1997; 71: 9065–74.
26. **Wang LH, Rothberg KG, Anderson RG.** Mis-assembly of clathrin lattices on endosomes reveals a regulatory switch for coated pit formation. *J Cell Biol*. 1993; 123: 1107–17.
27. **Sanchez-San Martin C, Lopez T, Arias CF, *et al.*** Characterization of rotavirus cell entry. *J Virol*. 2004; 78: 2310–8.
28. **Levitzki A, Willingham M, Pastan I.** Evidence for participation of transglutaminase in receptor-mediated endocytosis. *Proc Natl Acad Sci USA*. 1980; 77: 2706–10.
29. **Schlegel R, Dickson RB, Willingham MC, *et al.*** Amantadine and dansylcadaverine inhibit vesicular stomatitis virus uptake and receptor-mediated endocytosis of α2-macroglobulin. *Proc Natl Acad Sci USA*. 1982; 79: 2291–5.
30. **Orlandi PA, Fishman PH.** Filipin-dependent inhibition of cholera toxin: evidence for toxin internalization and activation through caveolae-like domains. *J Cell Biol*. 1998; 141: 905–15.
31. **Pelkmans L, Kartenbeck J, Helenius A.** Caveolar endocytosis of simian virus 40 reveals a new two-step vesicular-transport pathway to the ER. *Nature Cell Biol*. 2001; 3: 473–83.
32. **Popescu CI, Paduraru C, Dwek RA, *et al.*** Soluble tyrosinase is an endoplasmic reticulum (ER)-associated degradation substrate retained in the ER by calreticulin and BiP/GRP78 and not calnexin. *J Biol Chem*. 2005; 280: 13833–40.
33. **Eash S, Querbes W, Atwood WJ.** Infection of Vero cells by BK virus is dependent on caveolae. *J Virol*. 2004; 78: 11583–90.
34. **Bayer N, Schober D, Prchla E, *et al.*** Effect of bafilomycin A1 and nocodazole on endocytic transport in HeLa cells: implications for viral uncoating and infection. *J Virol*. 1998; 72: 9645–55.
35. **Richards AA, Stang E, Pepperkok R, *et al.*** Inhibitors of COP-mediated transport and cholera toxin action inhibit simian virus 40 infection. *Mol Biol Cell*. 2002; 13: 1750–64.
36. **Feng Y, Jadhav AP, Rodighiero C, *et al.*** Retrograde transport of cholera toxin from the plasma membrane to the endoplasmic reticulum requires the *trans*-Golgi network but not the Golgi apparatus in Exo2-treated cells. *EMBO Rep*. 2004; 5: 596–601.
37. **Connor J, Huang L.** Efficient cytoplasmic delivery of a fluorescent dye by pH-sensitive immunoliposomes. *J Cell Biol*. 1985; 101: 582–9.
38. **Bergstrand N, Arfvidsson MC, Kim JM, *et al.*** Interactions between pH-sensitive liposomes and model membranes. *Biophys Chem*. 2003; 104: 361–79.
39. **Huth US, Schubert R, Peschka-Süss R.** Investigating the uptake and intracellular fate of pH-sensitive liposomes by flow cytometry and spectral bio-imaging. *J Control Rel*. 2006; 110: 490–504.
40. **Connor J, Yatvin MB, Huang L.** pH-sensitive liposomes: acid-induced liposome fusion. *Proc Natl Acad Sci USA*. 1984; 81: 1715–8.
41. **Lubrich B, van Calker D, Peschka-Suss R.** Inhibition of inositol uptake in astrocytes by anti-sense oligonucleotides delivered by pH-sensitive liposomes. *Eur J Biochem*. 2000; 267: 2432–8.
42. **Fattal E, Couvreur P, Dubernet C.** "Smart" delivery of antisense oligonucleotides by anionic pH-sensitive liposomes. *Adv Drug Delivery Rev*. 2004; 56: 931–46.
43. **Lecot S, Belouzard S, Dubuisson J, *et al.*** Bovine viral diarrhea virus entry is dependent on clathrin-mediated endocytosis. *J Virol*. 2005; 79: 10826–9.
44. **Krey T, Thiel HJ, Rumenapf T.** Acid-resistant bovine pestivirus requires activation for pH-triggered fusion during entry. *J Virol*. 2005; 79: 4191–200.
45. **Mastrobattista E, Koning GA, van Bloois L, *et al.*** Functional characterization of an endosome-disruptive peptide and its application in cytosolic delivery of immunoliposome-entrapped proteins. *J Biol Chem*. 2002; 277: 27135–43.
46. **Nichols BJ.** A distinct class of endosome mediates clathrin-independent endocytosis to the Golgi complex. *Nat Cell Biol*. 2002; 4: 374–8.
47. **Rodal SK, Skretting G, Garred O, *et al.*** Extraction of cholesterol with methyl-β-cyclodextrin perturbs formation of clathrin-coated endocytic vesicles. *Mol Biol Cell*. 1999; 10: 961–74.
48. **Subtil A, Gaidarov I, Kobylarz K, *et al.*** Acute cholesterol depletion inhibits clathrin-coated pit budding. *Proc Natl Acad Sci USA*. 1999; 96: 6775–80.
49. **Zuhorn IS, Kalicharan R, Hoekstra D.** Lipoplex-mediated transfection of mammalian cells occurs through the cholesterol-dependent clathrin-mediated pathway of endocytosis. *J Biol Chem*. 2002; 277: 18021–8.
50. **Torgersen ML, Skretting G, van Deurs B, *et al.*** Internalization of cholera toxin by different endocytic mechanisms. *J Cell Sci*. 2001; 114: 3737–47.
51. **Kirkham M, Fujita A, Chadda R, *et al.*** Ultrastructural identification of uncoated caveolin-independent early endocytic vehicles. *J Cell Biol*. 2005; 168: 465–76.
52. **Kalia M, Kumari S, Chadda R, *et al.*** Arf6-independent GPI-anchored protein-enriched early endosomal compartments fuse with sorting endosomes via a Rab5/phosphatidylinositol-3'-kinase-dependent machinery. *Mol Biol Cell*. 2006; 17: 3689–704.
53. **Fretz MM, Koning GA, Mastrobattista E, *et al.*** OVCAR-3 cells internalize TAT-peptide modified liposomes by endocytosis. *Biochim Biophys Acta*. 2004; 1665: 48–56.
54. **Costin GE, Trif M, Nichita N, *et al.*** pH-sensitive liposomes are efficient carriers for endoplasmic reticulum-targeted drugs in mouse melanoma cells. *Biochem Biophys Res Commun*. 2002; 293: 918–23.
55. **Pollock S, Dwek RA, Burton DR, *et al.*** N-Butyldeoxynojirimycin is a broadly effective anti-HIV therapy significantly enhanced by targeted liposome delivery. *AIDS*. 2008; 22: 1961–9.